Lecture Notes in Civil Engineering

Pavel Akimov
Nikolai Vatin *Editors*

XXX Russian-Polish-Slovak Seminar Theoretical Foundation of Civil Engineering (RSP 2021)

Selected Papers

Springer

Lecture Notes in Civil Engineering

Volume 189

Lecture Notes in Civil Engineering (LNCE) publishes the latest developments in Civil Engineering - quickly, informally and in top quality. Though original research reported in proceedings and post-proceedings represents the core of LNCE, edited volumes of exceptionally high quality and interest may also be considered for publication. Volumes published in LNCE embrace all aspects and subfields of, as well as new challenges in, Civil Engineering. Topics in the series include:

- Construction and Structural Mechanics
- Building Materials
- Concrete, Steel and Timber Structures
- Geotechnical Engineering
- Earthquake Engineering
- Coastal Engineering
- Ocean and Offshore Engineering; Ships and Floating Structures
- Hydraulics, Hydrology and Water Resources Engineering
- Environmental Engineering and Sustainability
- Structural Health and Monitoring
- Surveying and Geographical Information Systems
- Indoor Environments
- Transportation and Traffic
- Risk Analysis
- Safety and Security

To submit a proposal or request further information, please contact the appropriate Springer Editor:

- Pierpaolo Riva at pierpaolo.riva@springer.com (Europe and Americas);
- Swati Meherishi at swati.meherishi@springer.com (Asia - except China, and Australia, New Zealand);
- Wayne Hu at wayne.hu@springer.com (China).

All books in the series now indexed by Scopus and EI Compendex database!

More information about this series at http://www.springer.com/series/15087

Pavel Akimov · Nikolai Vatin
Editors

XXX Russian-Polish-Slovak Seminar Theoretical Foundation of Civil Engineering (RSP 2021)

Selected Papers

Springer

Editors
Pavel Akimov
Moscow State University
of Civil Engineering
Moscow, Russia

Nikolai Vatin
Peter the Great St. Petersburg
Polytechnic University
Saint-Petersburg, Russia

ISSN 2366-2557 ISSN 2366-2565 (electronic)
Lecture Notes in Civil Engineering
ISBN 978-3-030-86000-4 ISBN 978-3-030-86001-1 (eBook)
https://doi.org/10.1007/978-3-030-86001-1

This Springer imprint is published by the registered company Springer Nature Switzerland AG
The registered company address is: Gewerbestrasse 11, 6330 Cham, Switzerland

Preface

Dear colleagues, participants of the XXX Russian-Polish-Slovak Seminar «Theoretical Foundation of Civil Engineering»!

This year, the Seminar is held within the framework of the «Year of Science and Technology» in the Russian Federation and dedicated to the 100th anniversary of Moscow State University of Civil Engineering.

Thirty years ago, a group of scientists from three neighbouring Slavic countries (occasionally from other countries also) organized the first Seminar «Theoretical Foundation of Civil Engineering». And for 30 years, scientists have been systematically meeting, alternately in Russia, Slovakia or Poland, on the occasion of the exchange of information in the scientific field of civil engineering. Every year, this Seminar becomes more and more popular.

This year, the organizers of the Seminar have become six universities: Moscow State University of Civil Engineering (MGSU); Wrocław University of Technology (WrUT); Don State Technical University (DSTU); University of Zilina (UNIZA); Warsaw University of Technology (WUT); Samara State Technical University (SamSTU).

Participants of the Seminar are not only representatives of universities–organizers, but also scientists from other research and educational institutions.

This year, the Seminar is held at Moscow State University of Civil Engineering (Moscow) and Samara State Technical University (Samara).

Seminar topics: Structural Mechanics; Building Structures; Geodesy and Geotechnics; Building materials and Technologies in Construction; Transport and Environmental Issues in Civil Engineering.

Special thanks should be given to our colleagues from the universities–co-organizers, who provided timely control over the preparation of papers and to the members of the international scientific committee, who promptly reviewed the papers.

The Russian-Polish-Slovak Seminar «Theoretical Foundation of Civil Engineering», which is being held for the thirtieth time, will once again confirm that meetings of scientists from different countries will expand our scientific potential, strengthen cooperation and friendship between us.

I wish all the participants of the Seminar successful presentations, further success in scientific activities, health and further meetings.

Pavel Akimov
Chairman

Contents

Building Structures

Dynamic Actions of a Two-Layer Freely Supported Beam

O. V. Ratmanova(✉) and M. A. Kalmova

Samara State Technical University, 244, Molodogvardeyskaya Street, 443100 Samara, Russian Federation

Abstract. The article deals with the issues of studying the stress-strain state of a structure presented in the form of a multilayer system made of various materials. A solution to the theory of elasticity and a classical solution based on Kirchhoff's hypotheses are presented. Formulas for determining the frequencies of free vibrations of the plate are determined. The results obtained are used in the construction of refined technical theories for the calculation of two-layer plates and shells. However, the problem that lies in the classical theory is significantly important, namely, this definition of the stress-strain state when a multilayer plate is investigated. The results obtained do not give any more accurate values that are required in the first place, but get an approximate solution, which significantly reduces the quality of the produced process. Thus, the developed calculation methodology is presented, which makes it possible to obtain accurate and high-quality calculations applicable for any number of layers and plate sizes.

Keywords: Bimorph plate · Kirchhoff theory · Theory of elasticity · Applied theory for thin plates

1 Introduction

In various multilayer structures, materials are used that differ in their physical and mechanical properties. This solution allows you to create elements with high elasticity and relatively low weight. However, the main advantage is high bending stiffness [1]. The problem is the study of the stress-strain state of elastic bimorph structures, which is carried out using the applied theory for thin plates, since they allow obtaining approximate results without delving into non-stationary processes. Thus, it is not possible to obtain a description of work in real conditions, and to solve this problem, it is proposed to use the theory of elasticity in a three-dimensional formulation [2–6].

For example, in [15], a calculation model is presented that gives an extended solution to the problem, satisfying all boundary conditions.

2 Formulation of the Problem

Consider the vibrations of a freely supported two-layer plate, infinitely long in the directional z-axis (Fig. 1). It is assumed that the layers of the plate are made of various isotropic materials and are glued in such a way that there is no slippage between them.

P. Akimov and N. Vatin (Eds.): RSP 2021, LNCE 189, pp. 3–9, 2022.
https://doi.org/10.1007/978-3-030-86001-1_1

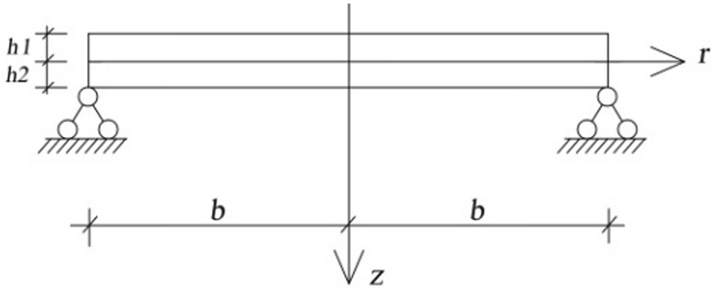

Fig. 1. Diagram of a two-layer plate.

In the general case, the differential equations of axisymmetric motion and boundary conditions in a cylindrical coordinate system in dimensionless form have the form:

$$\frac{\partial}{\partial r}\nabla U+\frac{C_{55}^{(s)}}{C_{11}^{(s)}}\frac{\partial^2 U}{\partial z^2}+\frac{\left(C_{13}^{(s)}+C_{55}^{(s)}\right)}{C_{11}^{(s)}}\frac{\partial^2 W}{\partial r\partial z}-^{(s)}\frac{\partial^2 U}{\partial t^2}=0$$

$$\frac{C_{55}^{(s)}}{C_{11}^{(s)}}\nabla\frac{\partial W}{\partial r}+\frac{C_{33}^{(s)}}{C_{11}^{(s)}}\frac{\partial^2 W}{\partial z^2}+\frac{\left(C_{13}^{(s)}+C_{55}^{(s)}\right)}{C_{11}^{(s)}}\frac{\partial}{\partial z}\nabla U-^{(s)}\frac{\partial^2 W}{\partial t^2}=0, \tag{1}$$

where $U(r_*, z_*, t_*)$, $W(r_*, z_*, t_*)$ - are the components of the displacement vector and the potential of the electric field in dimensional form; $\rho^{(s)}$, $C_{mk}^{(s)}$ – bulk density and elastic moduli of various materials; $\Phi^{(1)}=1$, $\Phi^{(2)}=\frac{C_{11}^{(2)}\rho^{(1)}}{C_{11}^{(1)}\rho^{(2)}}$, $\nabla=\frac{\partial}{\partial r}+\frac{1}{r}$.

$$r=0,1,\quad W(0,z,t)<\infty,\quad U(0,z,t)<\infty,\quad \phi(0,z,t)<\infty, \tag{2}$$

$$D_{r|r=1}=-\frac{C_{11}^{(1)}\varepsilon_{11}}{e_{33}^2}\frac{\partial\phi}{\partial r}+\frac{e_{15}}{e_{33}}\left(\frac{\partial W}{\partial r}+\frac{\partial U}{\partial z}\right)=0;$$

$z=0,h$

$$\sigma_{zz}=\frac{C_{13}^{(s)}}{C_{11}^{(1)}}\nabla U+\frac{C_{33}^{(s)}}{C_{11}^{(1)}}\frac{\partial W}{\partial z}=0,\ \sigma_{rz}=\frac{C_{55}^{(s)}}{C_{11}^{(1)}}\left(\frac{\partial W}{\partial r}+\frac{\partial U}{\partial z}\right)=0, \tag{3}$$

$$r=0,1\ \sigma_{rr|r=1}=\frac{C_{11}^{(s)}}{C_{11}^{(1)}}\frac{\partial U}{\partial r}+\frac{C_{12}^{(s)}}{C_{11}^{(1)}}\frac{U}{r}+\frac{C_{13}^{(s)}}{C_{11}^{(1)}}\frac{\partial W}{\partial z}=0$$

$$\sigma_{rz}=\frac{C_{55}^{(s)}}{C_{11}^{(1)}}\left(\frac{\partial W}{\partial r}+\frac{\partial U}{\partial z}\right)=0,$$

$$\sigma_{zz}=\frac{C_{13}^{(s)}}{C_{11}^{(1)}}\nabla U+\frac{C_{33}^{(s)}}{C_{11}^{(1)}}\frac{\partial W}{\partial z}=0,\ \sigma_{rz}=\frac{C_{55}^{(s)}}{C_{11}^{(1)}}\left(\frac{\partial W}{\partial r}+\frac{\partial U}{\partial z}\right)=0, \tag{4}$$

$$z = h_1, h_2$$
$$\frac{C_{13}^{(1)}}{C_{11}^{(1)}}\nabla U + \frac{C_{33}^{(1)}}{C_{11}^{(1)}}\frac{\partial W}{\partial z} + \frac{\partial \phi}{\partial z} = \frac{C_{13}^{(2)}}{C_{11}^{(1)}}\nabla U + \frac{C_{33}^{(2)}}{C_{11}^{(1)}}\frac{\partial W}{\partial z},$$
$$\frac{C_{55}^{(1)}}{C_{11}^{(1)}}\left(\frac{\partial W}{\partial r} + \frac{\partial U}{\partial z}\right) + \frac{e_{15}}{e_{33}}\frac{\partial \phi}{\partial r} = \frac{C_{55}^{(2)}}{C_{11}^{(1)}}\left(\frac{\partial W}{\partial r} + \frac{\partial U}{\partial z}\right),$$
$$U(z+0) = U(z-0),\ W(z+0) = W(z-0) \tag{5}$$

$$t = 0$$
$$U(r,z,0) = U_0(r,z),\ W(r,z,0) = W_0(r,z),$$
$$\frac{\partial U(r,z,t)}{\partial t}_{|t=0} = \dot{U}_0(r,z),\ \frac{\partial W(r,z,t)}{\partial t}_{|t=0} = \dot{W}_0(r,z) \tag{6}$$

3 General Solution Construction

The problems under consideration are solved by sequential use of the Hankel integral transforms with respect to the radial variable r and the generalized finite integral transform (GFA) along the axial coordinate z:

In this case, at each stage of the solution, the boundary conditions are standardized, that is, they are reduced to a form that allows the corresponding procedure for separating variables to be performed.

For this, with rigid fastening of the structure, the condition of the absence of vertical displacements of the cylindrical surface is replaced by the condition on this surface of the presence of tangential stresses $N_1(z,t)$:

$$\sigma_{rz|r=1} = N_1(z,t) \tag{7}$$

As a result, a new boundary value problem is formed, in which a known electrical load and unknown shear stresses act on the bimorph plate.

The procedure for bringing inhomogeneous boundary conditions is performed using the following expansion.

$$\{U, W\} = \{A_1, A_2\} + \{u, w\} \tag{8}$$

where A_1, A_2 – the reduction formulas.

As a result, the boundary conditions on the cylindrical surface of the plate are as follows:

$$w(1,z,t) = 0, \quad \nabla u_{|r=1} = 0, \quad \phi(1,z,t) = 0. \tag{9}$$

Applying successively the Hankel integral transformations (10), (11) and generalized finite integral transformations (12), (13) we obtain an expression for the components of the vector of displacement transformations and the potential of the electric field [7–9].

$$u_H(j_n,z,t) = \int_0^1 U(r,z,t) r J_1(j_n r) dr,\ w_H(j_n,z,t) = \int_0^1 w(r,z,t) r J_0(j_n r) dr \tag{10}$$

$$U(r,z,t) = 2\sum_{n=1}^{\infty}\frac{u_H(j_n,z,t)}{S(j_n)^2}J_1(j_n r),\ w(r,z,t) = 2\sum_{n=0}^{\infty}\frac{w_H(j_n,z,t)}{S(j_n)^2}J_0(j_n r) \quad (11)$$

$$G(\lambda_{in},n,t) = \int_0^h (U_H K_{1in} + W_H K_{2in})dz \quad (12)$$

$$\{U_H, W_H\} = \sum_{i=1}^{\infty} G_{in}\{K_{1in}, K_{2in}\}\|K_{in}\|^{-2},\ \|K_{in}\|^2 = \int_0^h \left(K_{1in}^2 + K_{2in}^2\right)dz \quad (13)$$

where λ_{in} −are parameters forming a countable set for each $n = \overline{0, \infty}$.

Dimensional circular frequencies of axisymmetric vibrations of the plate are determined by the formula:

$$\omega_{in} = \lambda_{in} b^{-1}\sqrt{C_{11}^{(2)}/\rho^{(2)}} \quad (14)$$

Approximate Solution

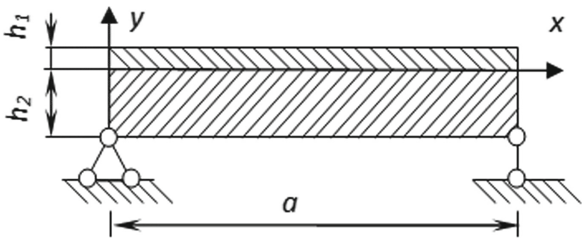

Fig. 2. Scheme of a two-layer plate for a classic setting

Consider an approximate solution to the previous problem in the classical formulation (based on Kirchhoff's hypotheses). If we take the neutral layer [10] as the initial plane and replace the transverse load with the amplitude value of inertial forces, then the equation of free vibrations of the plate can be written in the form

$$D_{np}\frac{d^4\omega}{dx^4} - (\rho_1 h_1 + \rho_2 h_2)\omega^2\omega = 0 \quad (15)$$

where D_{np}- is the reduced stiffness in bending of a two-layer plate relative to the neutral layer, equal to

$$D_{np} = 4(D_1 + D_2) - \frac{(B_1 h_1 - B_2 h_2)^2}{4(B_1 + B_2)} \quad (16)$$

Here D_i, B_i-determined by the formulas

$$D_i = \frac{E_i h_i^3}{12(1 - v_i^2)};\ B_i = \frac{E_i h_i}{1 - v_i^2}(i = 1, 2) \quad (17)$$

where E_i, v_i-Young's modulus and Poisson's ratio of the material of the i-th layer of the plate The boundary conditions of the problem for the edges $x = 0, a;\ \omega = \sigma_x = 0$ will be satisfied if we accept

$$\omega^2 = A \sin \alpha x;\ \alpha = \frac{n\pi}{a}\ (n = 1, 2, 3, \ldots) \tag{18}$$

Introducing (18) into Eq. (16), we obtain the formula for determining the frequency of free vibrations of the plate

$$\omega^2 = \frac{\alpha^4 D_{np}}{\rho_1 h_1 + \rho_2 h_2} \tag{19}$$

4 Conclusion

Calculations of the frequency of free vibrations were carried out for various elastic-geometric parameters of two-layer plates used by the classical theory.

Take steel ($E_1 = 2 \cdot 10^6\,\kappa\Gamma/\mathrm{cm}^2\ \upsilon_1 = 0,3$) and aluminum ($E_1 = 0,69 \cdot 10^6\,\kappa\Gamma/\mathrm{cm}^2\ \upsilon_1 = 0,34$), and for the lower layer-foams with elastic characteristics $E_2\ \upsilon_2$, equal to: $E_1 = 500; 2000; 3500; 600020000\ \kappa\Gamma/\mathrm{cm}^2$, $\upsilon_1 = 0,4; 0,4; 0,4; 0,3$ and plywood (with conditional isotropy) in which $E_2 = 1 \cdot 10^5\,\kappa\Gamma/\mathrm{cm}^2$). A bimitallic steel-aluminum plate is also considered and, for comparison, a homogeneous steel plate.

For each case, the frequencies were calculated at $\delta = \frac{h_2}{h_1}$ and half-wavelengths $l = \frac{a}{n} = 20, 100, 200$.

Total plate thickness $h = h_1 + h_2$ accepted 10 cm (Fig. 3).

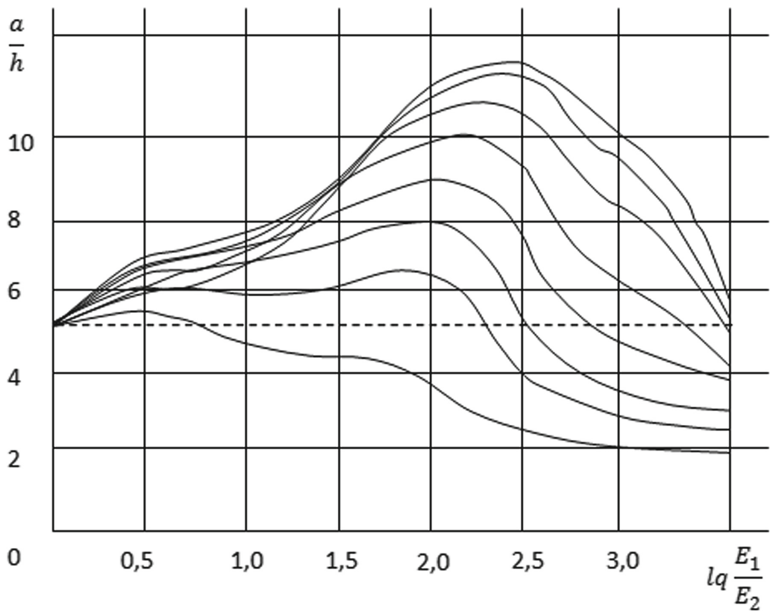

Fig. 3. Curves of relative half-wavelengths

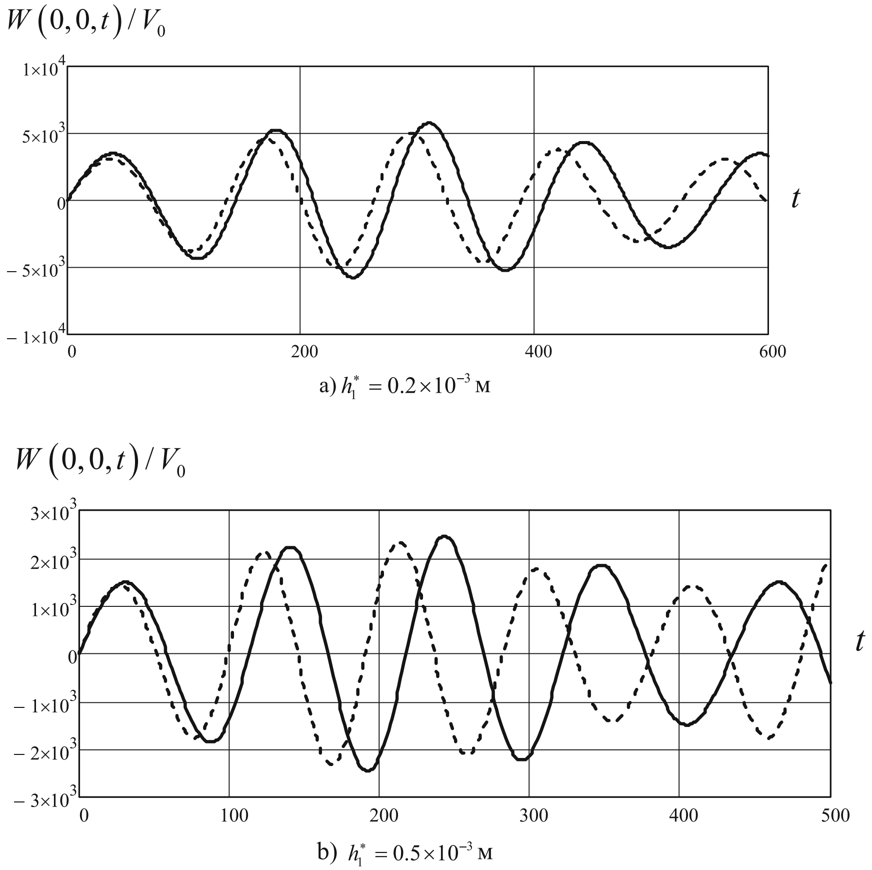

Fig. 4. Graphs of change over time

The resulting graphs in the developed theory, carried out through the Hankel transform, developed in the program MathCad (Fig. 4).

Thus, a method for calculating multilayer round bimorph plates has been developed, which allows using basic design ratios to describe their work in the case of loads. The problem is solved by the method of finite integral transformations, which, unlike the classical theory, is used in dynamic problems for finite bodies in time, does not require complex processing procedures.

References

1. Senitsky, Yu.E., Lytchev, S.A.: Three-layer spherical shells with asymmetrical layer structure and their dynamics, Building components and systems and their reliability. In: International Science Technical Conference Proceedings, Samara, pp. 67–71 (1997)
2. Grigoluk, E.I., Kulikov, G.M.: Elastic sandwich shells and multi-layer plates theory development. Vestnik TGTU **11**(2A), 439–448 (2005)

3. Demochkin, N.I., Morgachev, K.S., Fridman, L.I.: Timoshenko's model in cores and planes dynamics and its reliability. Proc. Russian Acad. Sci. **6**, 137–144 (2008)
4. Shlyakhin, D.A.: Forced axisymmetric vibrations of thin bi-morph plate. In: Proceedings of the Russian Academy of Sciences, pp. 77–85 (2013)
5. Shlyahin, D.A.: News of Russian Academy of Sciences. MTT **2**, 77–85 (2013)
6. Shlyakhin, D.A., Kazakova, O.V.: Proc. Eng. **91**, 69–74 (2014)
7. Senitskiy, Yu.E.: News of Saratov university, Series: Mat., Mech., Inform, **11,** 3 Part 1. (2011)
8. Shlyakhin, D.A.: Forced axisymmetric vibrations of a thick circular rigidly fixed piezoceramic plate. Vestnik Samara State Univ. Sci. **8**, 142–152 (2011)
9. Wang, Y., Xu, R.Q., Ding, H.J.: Analytical solutions of functionally graded piezoelectric circular plates subjected to axisymmetric loads. Acta Mech **215**, 287–305 (2010)
10. Korolev, V.I.: Thin double-layer plates and shells. Engineering collection, vol. XXII (1955)

Parametric Study of Saw-Cut Method

Jakub Kral'ovanec[1](✉), Martin Moravčík[1], Peter Koteš[1], and Andrej Matejov[2]

[1] Department of Structures and Bridges, Faculty of Civil Engineering, University of Žilina, Univerzitná 8215/1, 010 26 Žilina, Slovakia
jakub.kralovanec@uniza.sk

[2] Faculty of Civil Engineering, Department of Railway Engineering and Track Management, University of Žilina, Univerzitná 8215/1, 010 26 Žilina, Slovakia

Abstract. Knowledge of the level of residual prestressing is a crucial basis for determining the load-carrying capacity of prestressed concrete structures. The value of prestressing force decreases over time because of expected but sometimes also unexpected factors. Expected factors include prestress losses according to available standards. On the other hand, prestress losses that are not considered in standards can be attributed to environmental distress or conceptual problems of prestressed concrete structures. In Europe, we are challenging ageing infrastructure. Thus, we need to decide whether old bridges should be replaced, or their structural state facilitates to preserve them in service. The level of prestressing can be evaluated, e.g., using indirect methods for determining the value of residual prestressing force. These methods are based on the measurements of deflection, the width of the crack, or stress (strain) and subsequently, it is possible to determine the actual state of prestressing indirectly using obtained results. This paper introduces the parametric study of Saw-cut method which is generally considered as a non-destructive indirect method. A presented study is performed for the determination of factors that could influence the application of Saw-cut methods in practice. The studied factors include the value of prestressing force, depth and axial distance of saw-cuts, and FE mesh. For numerical analysis, a 2D finite element model with the assumption of nonlinear material behavior is performed in ATENA 2D Software. Finally, the conclusions of the parametric study are discussed and summarized.

Keywords: Saw-cut method · Prestressed concrete · Parametric study · Assessment · Prestress losses

1 Introduction

In the early 1960s in former Czechoslovakia, precast and prestressing technologies have started to be commonly used [1, 2]. As the first precast post-tensioned bridges in Slovakia are now approaching 60 years of service life, it is necessary to assess their present structural condition and residual life expectancy [3]. Furthermore, significant information about the long-term behavior of structures should be collected for these reasons [4]. In the case of prestressing steel, usage of magnetic Barkhausen noise (MBN) can

P. Akimov and N. Vatin (Eds.): RSP 2021, LNCE 189, pp. 10–19, 2022.
https://doi.org/10.1007/978-3-030-86001-1_2

offer an effective tool for its assessment [5–7] as insufficient inspection and neglected maintenance can result in the need for intervention and the decision to close the bridge. In these cases, the safety of the structure is endangered and demountable temporary bridges must be installed what consequently leads to the additional cost for the operator [8]. Existing bridges are structures that reflect not only the level of the society in which they were built but also the cultural and economic power of present generations, as they reflect the care for these inherited engineering works [9].

The value of the prestressing force decreases over time. Available standards for the design of prestressed concrete structures offer an approach for the calculation of expected short-term and long-term prestress losses. Standards take into account construction stages, methods of prestressing, and expected service life of the prestressed concrete structure. However, practice shows that sometimes the level of prestressing of prestressed structures in service is lower than the theoretically determined value. Additional prestress losses above value determined according to standards can be attributed to the degradation of materials caused by environmental distress, for example, corrosion of prestressing steel or decrease of the bond between prestressing steel and concrete. Thus, the need for reliable methods for determining the actual state of prestressing becomes more important. A pivotal object of this paper is the stress (strain) release method called Saw-cut method. This method is classified as the indirect non-destructive method, as it has only a negligible impact on the investigated prestressed concrete structure and its integrity is preserved. Stress release methods are based on intervention into the structure which causes a change in stress in the monitored area. In addition to the already mentioned Saw-cut method, this group of methods include, for example, Drilling method which is also called Stress-relief coring technique. On one hand, in the case of Saw-cut method, the stress relief is caused by the application of two or more saw-cuts. On the other hand, Drilling method is based on drilling a small hole into the concrete structure. Saw-cuts fully or partially isolate concrete block from the acting forces. Recorded change in stress (strain) enables evaluation of the value of residual prestressing force based on knowledge of load applied on investigated structure in the time of the test [10–13]. This paper deals with the parametric study which should provide important information about factors that could influence the application of Saw-cut method and offer an important basis for its later experimental verification (Fig. 1).

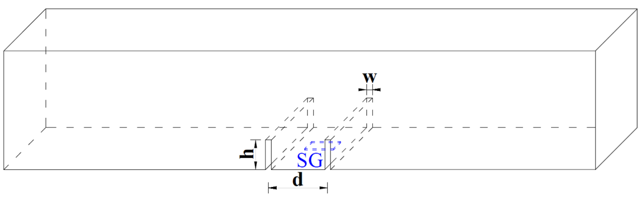

Fig. 1. Saw-cut method.

2 Numerical Analysis

The object of the presented parametric study is a post-tensioned concrete beam with a length of 4.20 m and a rectangular cross-section of 0.20 × 0.40 m which is designed from the concrete strength class of C30/37. An analyzed post-tensioned concrete beam is shown in Fig. 2. The prestressing tendon consists of a 15.7 mm strand placed in a duct with a diameter of 48 mm which is fully injected with cement grout. Consequently, prestressing is transferred through both the build-in anchor and the bond between steel and concrete. Conventional reinforcement of beam includes two B500B 10 mm bars at the bottom and two at the top. Moreover, in the edges of the beam, U shape bars of 6 mm, are placed longitudinally and transversally. Shear reinforcement of beam is provided by 6 mm two-legged stirrups with a maximum spacing of 0.20 m. Material properties used in numerical analysis are listed in Table 1.

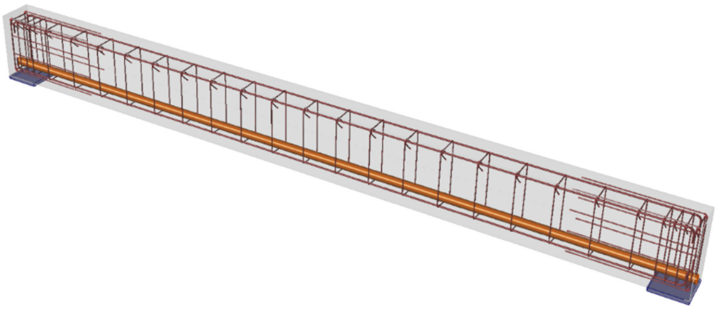

Fig. 2. Axonometric view on beam's reinforcement.

Table 1. Material properties of macro-elements used in a 2D numerical model.

Description	Material type	E [GPa]	Other properties
Post-tensioned beam	SBeta	33.01	$f_{cu} = 37.0$ MPa $f_c = 31.45$ MPa $f_t = 2.665$ MPa $\nu = 0.20$
Conventional reinforcement	Reinforcement - Bilinear	200.0	$f_y = 500.0$ MPa
Prestressing steel		195.0	$f_y = 1660.0$ MPa
Steel plates	Plane Stress Elastic Isotropic	210.0	$\nu = 0.30$
Saw-cuts		1.0×10^{-6}	$\nu = 0.30$

A 2D numerical analysis with the assumption of nonlinear behavior was performed in ATENA 2D Software (version ATENA 5.7.0n, Červenka Consulting, Prague, Czech Republic) [14–17]. Saw-cut method was applied on the precast post-tensioned concrete beam which was described above. The beam in question was loaded only by dead load and prestressing, while the analysis was provided using the Newton-Raphson method. In the numerical model, the analyzed beam was supported by two steel plates with dimensions 0.20 × 0.20 × 0.02 m. Consequently, the supports represented by steel plates were located at the bottom at an axial distance of 4.0 m which also correspond to the effective span of a simply supported beam. The numerical model is shown in Fig. 3.

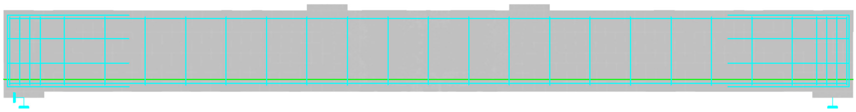

Fig. 3. 2D Numerical model in ATENA Software.

In the 2D numerical analysis, the application of the saw-cuts was modelled using "construction stages". In the first stage, all macro-elements were assigned the properties of the beam's concrete. In the next stage, the modulus of elasticity of the macro-elements that represented the saw-cuts was changed. Hence, considering the sawing of the beam. The stress monitoring point was placed in the middle of the effective span and axial distance of saw-cuts at the bottom of the post-tensioned beam. The saw-cuts were modelled with a width of 5 mm.

The SBeta constitutive model of concrete includes 20 material parameters. These parameters were based on Eurocode 2 [19] and guidelines for FE analysis of concrete structures in ATENA Software. The formulation of constitutive relations was considered in the plane stress state. The concept of the material model SBeta includes the non-linear behavior in compression; the fracture of concrete under tension, based on the non-linear fracture mechanics biaxial strength failure criterion; a reduction in compressive strength after cracking; the tension stiffening effect; a reduction in the shear stiffness after cracking; and two crack models (the fixed crack direction and rotated crack direction) [14–17].

2.1 Value of Prestressing Force

In the parametric study, the influence of two different values of prestressing force (P = 61.7 and 145.0 kN) was studied. These values were determined based on the real measured prestressing force in prestressed concrete specimens at the time of tensioning of post-tensioned beams which are numerically analyzed, and in the future, they will be experimentally tested. Subsequently, these values were reduced by expected prestress losses according to Eurocode 2 [18] until the moment of expected experimental testing (365 days). The calculated percentage values of stress change ($\Delta\sigma_c$) at the monitored point between saw-cuts can be seen in Fig. 4. In order to demonstrate observed relations, only the results for an axial distance of saw-cuts (d) of 100 mm and FE Mesh 1 are presented.

2.2 Finite Element Mesh

Undoubtedly, the choice of size and kind of FE mesh has a significant impact on the obtained results from numerical models. For this reason, three different FE meshes were

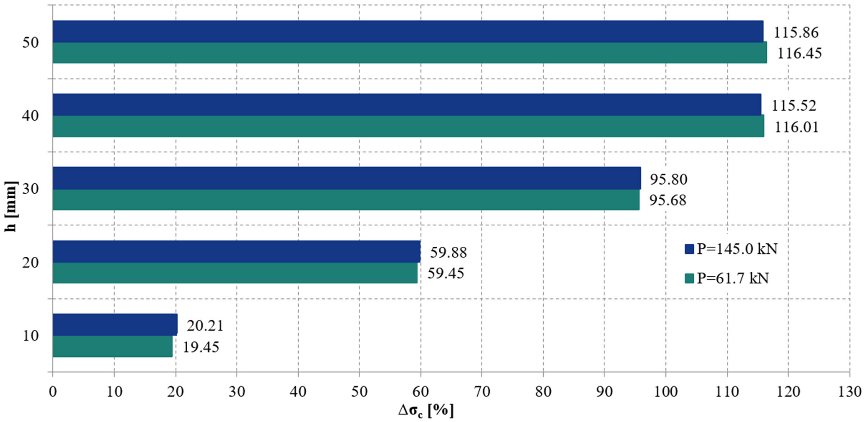

Fig. 4. Stress change for two different values of the prestressing force (d = 100 mm; FE Mesh 1).

analyzed in this study. In all three cases, the FE mesh was generated automatically according to defined element size using quadrilateral CCQ10SBeta elements implemented in ATENA 2D Software. First, the relatively large size of FE elements was defined, see Fig. 5a. All macro-elements were composed of elements with a uniform size of 50 mm. Second, in the middle area of the post-tensioned beams, at a width of 300 mm and height of 70 mm (the area adjacent to the saw-cuts), the mesh was smoothed into elements with a size of 5 mm. The rest of the modelled beams was composed of elements with a uniform size of 50 mm, the same as in the FE Mesh 1. FE Mesh 2 can be seen in Fig. 5b. Third, in the middle area of the post-tensioned beam, at a width of 700 mm and height of beam's cross-Sect. (400 mm) the mesh was smoothed into elements with a size of 10 mm. The rest of the modelled beam was composed of elements with a uniform size of 50 mm, see Fig. 5c. In the case of all analyzed FE meshes, saw-cuts' macro-elements were smoothed into elements with a size of 5 mm.

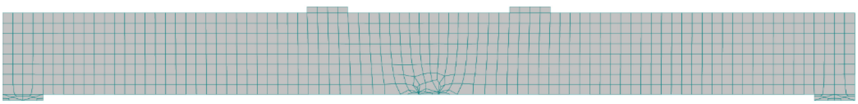

(a)

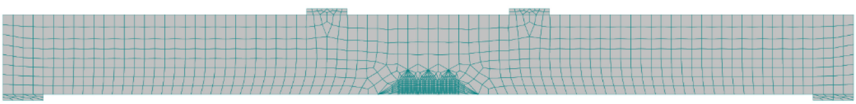

(b)

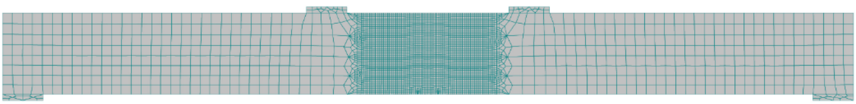

(c)

Fig. 5. (a) FE Mesh 1; (b) FE Mesh 2; (c) FE Mesh 3.

Results from the numerical analysis suggest that FE Mesh 1 with relatively large size of elements provide a large discrepancy in comparison with the other two analyzed FE meshes. This fact is significant, especially for deeper saw-cuts. The stress relief ($\Delta\sigma_c$) differences between FE Mesh 2 and FE Mesh 3 for all depth of saw-cuts are negligible. Results are presented in Fig. 6.

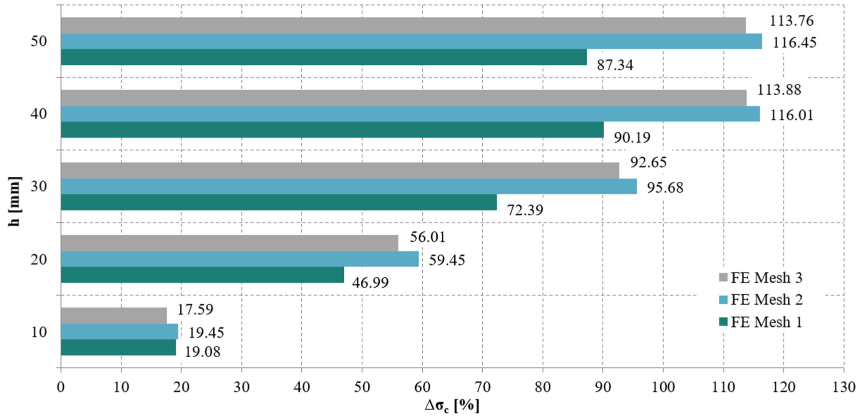

Fig. 6. Stress change for three different types of FE mesh (P = 61.7 mm; d = 100 mm).

2.3 Parameters of Saw-Cuts

In parametric study, saw-cuts' depths (h) of 10; 20; 30; 40 and 50 mm were considered. The analysis of saw-cuts' depth influence on stress relief in monitored point was performed for six different axial distances from 100 to 150 mm. It appears that full isolation of concrete block from the acting forces could be reached for saw-cuts in the

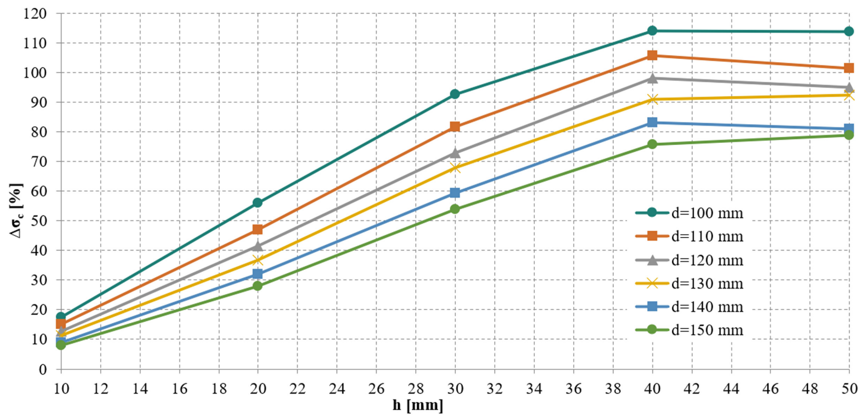

Fig. 7. Relation between stress change and saw-cuts' depth – constant axial distance.

axial distance of 120 mm or less. The relation between stress relief ($\Delta\sigma_c$) and depth of saw-cuts (h) is shown in Fig. 7.

In addition to analysis of the influence of depth of saw-cuts, axial distances (d) of 100; 110; 120; 130; 140 and 150 mm were studied too. The relation between stress relief ($\Delta\sigma_c$) and the axial distance (d) of saw-cuts is presented in Fig. 8.

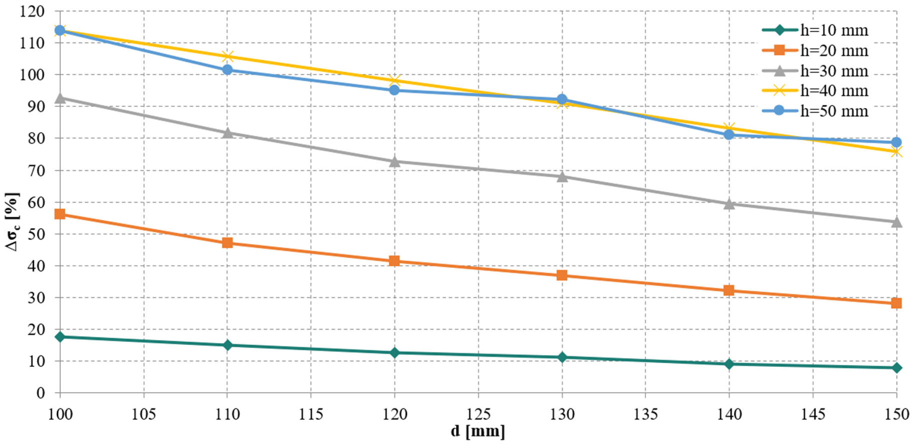

Fig. 8. Relation between stress change and saw-cuts' axial distance – constant depth.

3 Discussion

It is evident that both, axial distance and depth of saw-cuts, significantly influence stress relief and thus they are the only important factors in Saw-cut method. Presented relations describe the change in stress in the monitored point for one variable parameter and one constant parameter of saw-cuts. However, final stress relief ($\Delta\sigma_c$) is influenced simultaneously by both parameters. Therefore, the relation taking into account the effect of depth and axial distance of saw-cuts was derived in Eq. 1. Regression analysis was performed using so-called Surface Fitting.

$$\Delta\sigma_c[\%] = 18.634617 \times h\,[mm] - 0.149179 \times h\,[mm]^2 - 6.303982 \times \ln(d\,[mm]) \times \ln^2(h\,[mm]) \quad (1)$$

Figure 9a presents the results of regression analysis based on the numerical analysis. The red surface represents the relation between stress change and saw-cuts' parameters according to Eq. 1. Moreover, it can be seen the comparison between regression and numerical analysis (grey points). Percentage stress relief iso-areas are displayed in Fig. 9b.

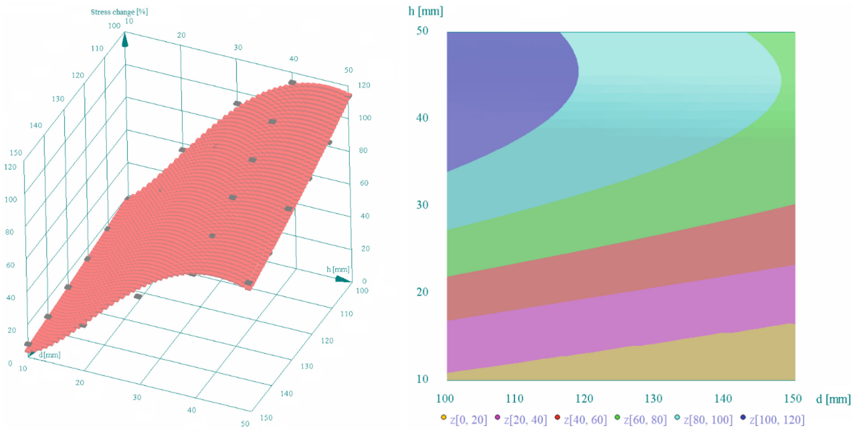

(a) (b)

Fig. 9. Evaluation of parametric study – (a) Surface Fitting; (b) stress change for saw-cuts' parameters according to the equation based on Surface Fitting.

4 Conclusions

Based on the performed numerical analysis, the following conclusions can be summarized:

It can be stated that the initial value of the prestressing force (P) does not influence percentage stress relief ($\Delta\sigma_c$) after the application of saw-cuts. We reached the same conclusions also in the case of all studied parameters (h and d) of saw-cuts and FE meshes of the numerical model. Consequently, it is not necessary to consider the value of the prestressing force (initial stress) as a factor that affects the rate of isolation of concrete block from the acting forces.

A study of FE mesh influence suggests that for numerical analysis of Saw-cut method, it is suitable to use at least locally smoothed FE mesh.

Deeper saw-cuts with shorter axial distance cause a higher rate of isolation of concrete block from the acting forces. A full stress change of 100% can be expected for saw-cuts in an axial distance of 120 mm or less simultaneously with a depth of 40 mm or more. Saw-cuts with a depth of 30 mm in an axial distance of 100 mm could produce almost 100% of stress change, which should be a practically sufficient rate of stress relief too.

The relation between the depth of saw-cuts from 10 to 40 mm and stress change seems to be approximately linear. Nevertheless, the discrepancies of stress relief for a depth of 50 mm can be attributed to sufficient isolation of concrete block a thus the percentage rate of stress change reaches its maximal value. Eventually, concrete cover in the case of old prestressed concrete structures can be low in compliance with today standards [18], hence such deep saw-cuts have only limited applicability in practice.

This parametric study offers an important basis for the application of Saw-cut method in laboratory and in situ tests. Indirect stress release methods can grow to be a useful and cheap tool for engineers in practice. In the coming decades, the determination of the residual level of prestressing is likely to become a crucial aspect in the structural assessment of existing prestressed concrete structures in service. In practical application, the saw-cuts' parameters should be chosen with respect to the position of structures' reinforcement (concrete cover) and used the length of the strain gauge's measuring grid. Future research should focus on the verification of conclusions introduced in this parametric study. Given that the presented findings are based on a limited number of performed FE simulations, the results from such a study should, therefore, be treated with considerable caution and inevitably experimentally verified.

Acknowledgements. This research project was supported by the Slovak Grant Agency under contracts No. 1/0045/19 and No. 1/0306/21 and by the Grant System of the University of Žilina under contract No. 7957.

References

1. Bujňáková, P., Strieška, M.: Development of precast concrete bridges during the last 50 years in Slovakia. In: International scientific conference on sustainable, modern and safe transport. TRANSCOM 2017. Procedia Engineering, vol. 192, pp. 75–79 (2017). https://doi.org/10.1016/j.proeng.2017.06.013.
2. Halvonik, J., Borzovic, V., Paulik, P.: Slab-on-girder bridges in Slovakia. In: Proceedings of the International fib Symposium on Conceptual Design of Structures, pp. 113–120, Madrid, Spain (2019)
3. Bujňáková, P.: Anchorage system in old post-tensioned precast bridges. Civil Environ. Eng. **16**, 379–387 (2020). https://doi.org/10.2478/cee-2020-0038
4. Bujnak, J., Bujnakova, P., Jedraszak, B.: Modelling and verification of bridge behaviour. MATEC Web Conf. **174**, 03002 (2018). https://doi.org/10.1051/matecconf/201817403002
5. Neslušan, M., Bahleda, F., Trojan, K., Pitoňák, M., Zgútová, K.: Barkhausen noise in overstressed wires. J. Magn. Magn. Mater. **513**, 167134 (2020). https://doi.org/10.1016/j.jmmm.2020.167134
6. Neslušan, M., Bahleda, F., Minárik, P., Zgútová, K., Jambor, M.: Non-destructive monitoring of corrosion extent in steel rope wires via Barkhausen noise emission. J. Magn. Magn. Mater. **484**, 179–187 (2019). https://doi.org/10.1016/j.jmmm.2019.04.017
7. Šrámek, J., Neslušan, M., Bahleda, F., Zgútová, K., Schenk, P.: Influence of sample size and magnetizing voltage on Barkhausen noise during bending and uniaxial tensile test. Acta Phys. Polonica A **137**, 640–643 (2020). https://doi.org/10.12693/APhysPolA.137.640
8. Vičan, J., Farbák, M.: Analysis of high - strength steel pin connection. Civil Environ. Eng. **16**, 276–281 (2020). https://doi.org/10.2478/cee-2020-0027
9. Gocál, J., Odrobiňák, J.: On the influence of corrosion on the load-carrying capacity of old riveted bridges. Materials **13**, 717 (2020). https://doi.org/10.3390/ma13030717
10. Kral̆ovanec, J., Moravčík, M.: Numerical verification of the saw-cut method. In: 2021 IOP Conference Series: Materials Science and Engineering, vol. 1015, p. 012031 (2021). https://doi.org/10.1088/1757-899X/1015/1/012031
11. Kral̆ovanec, J., Moravčík, M., Bujňáková, P., Jošt, J.: Indirect determination of residual prestressing force in post-tensioned concrete beam. Materials **14**, 1338 (2021). https://doi.org/10.3390/ma14061338
12. Bagge, N., Nilimaa, J., Elfgren, L.: In-situ methods to determine residual prestress forces in concrete bridges. Eng. Struct. (2017). https://doi.org/10.1016/j.engstruct.2016.12.059
13. Bagge, N., Nilimaa, J., Blanksvärd, T., Elfgren, L.: Instrumentation and full-scale test of a post-tensioned concrete bridge. Nordic Concr. Res. **51**, 63–83 (2014)

14. Červenka, V., Jendele, L., Červenka, J.: ATENA Program Documentation – Part 1. Theory. Prague (2018). https://www.cervenka.cz/assets/files/atena-pdf/ATENA_Theory.pdf
15. Červenka, V., Červenka, J.: ATENA Program Documentation – Part 2–1. User's Manual for ATENA 2D. Prague (2015). https://www.cervenka.cz/assets/files/atena-pdf/ATENA-Engineering-2D_Users_manual.pdf
16. Červenka, J.: ATENA Program Documentation – Part 4–1. Tutorial for Program ATENA 2D. Prague (2015). https://www.cervenka.cz/assets/files/atena-pdf/ATENA-Engineering-2D_Tutorial.pdf
17. Janda, Z., Červenka, J.: ATENA Program Documentation – Part 4–3. Tutorial for Construction Process Modelling in ATENA 2D. Prague (2009). https://www.cervenka.cz/assets/files/atena-pdf/ATENA-Engineering-2D_Tutorial_Construction_Process.pdf
18. Eurocode 2: Design of Concrete Structures—Part 1–1: General Rules and Rules for Buildings; STN EN 1992–1–1+A1; Slovak Technical Standard; Slovak Office of Standards, Metrology and Testing: Bratislava, Slovakia (2015)